Modelling of phase-grating based wideband tuneable lasers with simplified quasi-digital wavelength selection

A.J. Ward, D.J. Robbins, G. Busico, N.D. Whitbread, P.J. Williams, D.C.J. Reid and J.R. Rawsthorne

Abstract: A transfer matrix based model is discussed which was used to simulate a novel wideband tuneable laser design. This model can simulate the predicted behaviour of an arbitrary, multi-section distributed Bragg reflector (DBR) laser and can successfully predict tuning behaviour, threshold current, output power and static side-mode suppression ratio. The particular DBR laser, the digital super-mode DBR (DS-DBR), tunes by means of a highly uniform comb of narrow reflection peaks coupled with a multi-grating structure that can be used to digitally select a sub-band of the total tuning range. By selecting sub-bands in turn, the whole tuning range of the device can be accessed. Results of the model are compared with experimental results for this device which show a tuning range of around 50 nm, together with output powers in the range 8–9 dBm and a side-mode suppression ratio of better than 50 dB over 80 WDM channels at 50 GHz spacing. These results are for a device packaged in a standard 26-pin butterfly module.

1 Introduction

Widely tuneable InP lasers can, in principle, cover one or other of the Er-doped fibre amplifier windows and have been acknowledged as a key component for future DWDM communication systems [1]. However, the change in refractive index that can be achieved by current injection into a grating section is limited to about 1–2% corresponding to around 10 nm in wavelength terms, so some further mechanism is required to extend the tuning range. One strategy is to use a comb reflector with several reflection peaks at one end of the laser device and then use some means of selecting one of those peaks. By selecting different peaks in turn the total tuning range of the device can be enhanced by a factor equal to the number of reflection peaks used. One way to do this is by vernier tuning two different grating combs [2, 3]. Vernier-tuned devices typically require multidimensional current control algorithms for wavelength selection.

In this paper, we present a new multi-section DBR laser that can be controlled in a simple, quasi-digital manner. The wavelength can be coarsely selected by applying current to one or more of the front contacts to form an enhanced reflection peak and select a sub-band of the total tuning range. Current applied to the rear grating contact allows tuning within that range and a phase section allows fine tuning control. By selecting front contacts in turn, the full tuning range of the device can be accessed. The successful operation of this novel tuning mechanism depends critically on the top-hat shape of the reflection comb produced by the rear reflector. In the present device the rear reflector is a phase grating [4].

Our multi-section DBR device has been modelled using a transfer matrix based approach that can calculate threshold current and lasing wavelength for any applied set of tuning currents. The model can also estimate other important quantities such as output power and static side-mode suppression ratio and is applicable to any multi-section, integrated, semiconductor DBR laser. Using this tool we were able to predict the operation of the laser and explore some of its design space before any actual devices were made. We present initial experimental results showing single-mode behaviour with a high side-mode suppression ratio and wide tuning range in excellent agreement with the predicted tuning.

2 Design issues

In this paper we describe a new four-section device consisting of front and rear gratings, a gain section and a phase section [5]. A schematic of this device is shown in Fig. 1. The rear grating provides a comb reflector, whilst the front grating consists of a series of very short gratings of different pitches each with its own electrical contact. In the absence of current the front reflector provides a spectrally broad reflection with little modal discrimination. When a current is applied to one of the front contacts, the change in refractive index induced is sufficient to shift its Bragg wavelength to coincide with the Bragg wavelength of its shorter wavelength neighbour. This produces an enhanced reflection peak at a particular wavelength (Fig. 2). Since the gratings are short, this enhanced reflection peak can be

IEE Proceedings online no. 20030315

DOI: 10.1049/ip-opt:20030315

Paper first received 2nd July and in revised form 13th November 2002

The authors are with Bookham Technology, Caswell, Towcester, Northants, NN12 8EQ, UK

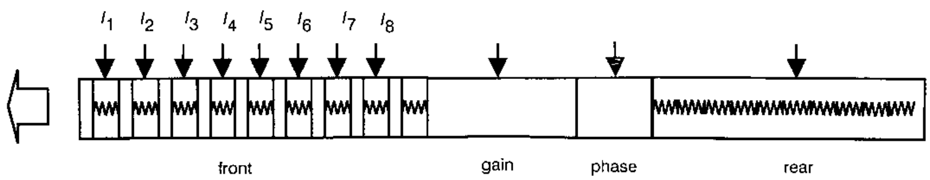

Fig. 1 *Schematic of the DS-DBR concept (not to scale)*

spectrally rather broad and it effectively selects a sub-band of the total tuning range by picking out one and only one of the narrow peaks from the comb reflector at the other end of the device. Tuning within this sub-band is possible by injecting current into the rear grating. Through the correct choices of pitches for the short front gratings it is possible to select different, overlapping tuning sub-bands by simply injecting current into different parts of the front grating structure.

In order for this novel tuning mechanism to work successfully the comb reflector needs to consist of peaks of approximately the same height. In practice, the peak height variation must be less than 1–2 dB since the enhancement that can be obtained by adding gratings together at the front of the device is clearly at best a factor of two and the magnitude of the gain across the tuning band will show some variation. With this limitation in mind a suitable choice is a phase grating, which consists of a number of lengths of uniform grating separated by π-phase shifts [4]. By choosing the correct lengths for the gratings between the phase shifts, the spectral response of the grating can be tailored into a comb reflector consisting of a number of equally spaced peaks of almost equal heights and very small spurious peaks (Fig. 2).

This new design offers several advantages over alternative approaches. First, the total current that needs to be injected into the front section to form a reflection peak is small. This is because at any one time we only pump a small part of the complete front grating structure. In turn this leads to less free-carrier absorption and less variation in output power as the device is tuned. Secondly, the control of the device is in principle rather simple since it is quasi-digital. That is to say that once the front tuning currents have been applied to select a tuning sub-band, the width of the front grating reflection is sufficient that the operating wavelength is defined by the rear grating (and phase section). Therefore, high accuracy in the front grating tuning is unnecessary.

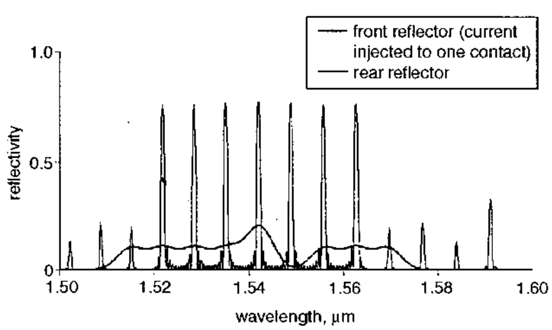

Fig. 2 *Diagram showing the front and rear reflector responses*
An enhanced peak is formed in the front reflector by injecting current to select a tuning sub-band. The exact lasing wavelength is determined by the rear reflector

3 Theory

The approach that we have used to model the DS-DBR device is the transfer matrix method [6]. This simple yet powerful frequency-domain method has been applied to a wide range of problems, including the modelling of photonic crystals [7] and low energy electron diffraction [8]. In general, the transfer matrix method can analyse the response of an arbitrary three-dimensional scatterer, but in the context of a single-mode laser waveguide we can reduce the problem to a one-dimensional case. In this instance the transfer matrix is simply a (2×2) matrix which relates the amplitudes of the forwards and backwards propagating waves at $(\boldsymbol{r})$ with the amplitudes at $(\boldsymbol{r}+\boldsymbol{c})$. If we divide our laser structure up into a number of simple, discrete sections for which we can find the transfer matrices, then the transfer matrix for the complete laser is given as the product of the matrices for the individual parts. We can therefore relate the forwards and backwards travelling waves at one end of the device to those at the other end (Fig. 3). (Note that the transfer matrices for different laser sections are found by coupled-mode theory [9]. For a detailed discussion including explicit forms for the matrices see [10]). For the purposes of analysing the basic tuning behaviour of our DS-DBR laser, a static, near threshold model is sufficient even though this neglects effects such as longitudinal spatial hole burning which may become important at higher currents. In this case, a single matrix can be used to describe each part of the laser which is homogeneous in terms of its material parameters or injected current. This leads to a very efficient description of the device and rapid simulation times.

As inputs into the model we must provide information on the material gain as a function of wavelength and injected current, and also the refractive index and loss of the tuning sections as a function of injected current and wavelength. In all of these, we have taken the view that the best approach is an empirical one, so the functional forms for these parameters have been obtained by fitting to experimental data and applying interpolation where necessary. Figs. 4–6 show typical curves for gain, loss and refractive index shift as well as the experimental data points to which they were fitted, as used in the model. The data for the material gain were obtained from Hakki–Paoli measurements [11] taken on Fabry–Perot devices fabricated from the same material as the gain sections of our DS-DBR lasers. The measured gain curves have been fitted to a parameterised, parabolic form with a logarithmic dependence of the peak gain on injected current density

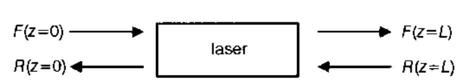

Fig. 3 *Diagram showing the forwards and backwards propagating waves at either end of a laser structure*

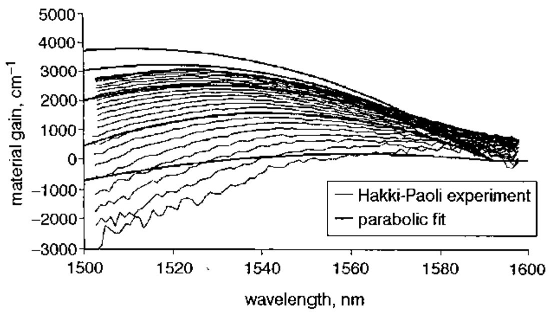

Fig. 4 *Measured material gain data and the fitted curves used in the transfer matrix model*

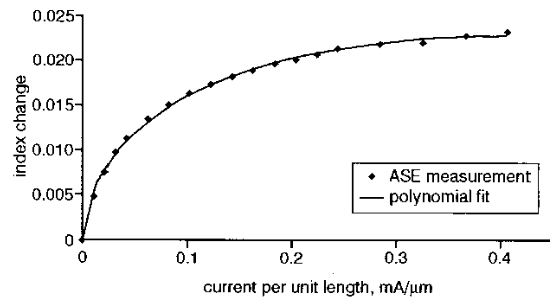

Fig. 6 *Measured data for the change in refractive index in the tuning sections with injected current and the fitted curve used in the transfer matrix model*

(see for example [12]). Fig. 5 shows the excess loss (the additional loss caused by the injected tuning current) within the tuning sections. The background loss (not shown in the Figure) is small and measurements have shown it to be of the order of a few per centimetre. In the modelling work we have assumed a value of $5\,\text{cm}^{-1}$. Waveguide loss can be measured in a variety of ways but one simple method is to use specially designed test structures which allow one to measure the transmission of generated light through two different passive waveguides, one of length L and another of length $2L$. By comparing the transmitted powers, the waveguide loss can be deduced.

Other physical parameters used in the model are given in Table 1.

Once we have found the complete transfer matrix for the laser then we can go on to find the threshold condition. At threshold, the out-going fields ($F(L)$ and $R(0)$) will be finite whilst the in-coming fields ($F(0)$ and $R(L)$) remain zero. If T_{ij} are the transfer matrix elements for the complete structure then

$$\begin{pmatrix} F(L) \\ R(L) \end{pmatrix} = \begin{pmatrix} T_{11} & T_{12} \\ T_{21} & T_{22} \end{pmatrix} \cdot \begin{pmatrix} F(0) \\ R(0) \end{pmatrix}$$
$$F(0) = R(L) = 0 \qquad (1)$$
$$F(L) = T_{12}R(0)$$
$$0 = T_{22}R(0)$$

Hence

$$T_{22} = 0 \qquad (2)$$

In order to find the threshold point of the laser we must therefore search over the dependent variables of the transfer matrix (wavelength and injected gain current in our case) to find the points where $T_{22} = 0$. This set will

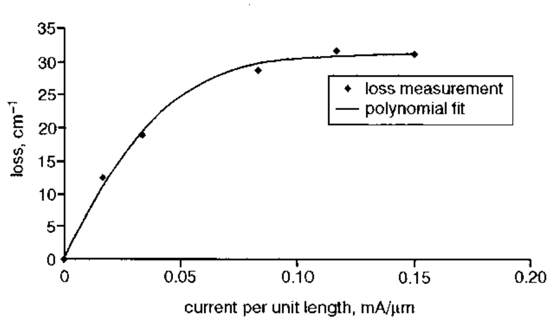

Fig. 5 *Measured data for the change of loss in the tuning sections with injected current and the fitted curve used in the transfer matrix model*

correspond to all the possible modes of the laser, and the one with the lowest gain current will be the actual lasing mode. In practice, this search is non-trivial because of the potentially wide wavelength range the laser can tune over, coupled with the high accuracy required to locate the cusp-like minima of T_{22}. We overcome this by applying what we know about the intended device behaviour to narrow the search before we start. Since it is intended that the tuning of the laser is controlled by the reflection peaks, then we can begin by scanning coarsely over the full wavelength tuning range to find places where the product of the reflectivities of the front and rear reflectors is large. These reflection peaks will be fairly narrow but still contain several longitudinal modes. We can, though, estimate the longitudinal mode spacing from the device geometry and divide the reflection peak up into enough subsections that we can be sure that each subsection contains at most only one longitudinal mode. A local minimisation algorithm applied to each section in turn can then efficiently locate each mode.

Table 1: Key physical parameters used in modelling our DS-DBR structure

Parameter	Value
Gain section length (μm)	600.0
Phase section length (μm)	150.0
Total front grating structure length (μm)	225.0
Rear grating comb spacing (nm)	6.8
Drive current for power calculation (mA)	300.0
Laser heat sink temperature (°C)	25.0
Laser ridge width (μm)	2.0
Laser thickness (μm)	100
Thermal conductivity ($\text{W K}^{-1}\,\mu\text{m}^{-1}$)	6.80×10^{-5}
Threshold current T_0 at room temperature (K)	64.0
Threshold current T_0 at temperature > 41°C (K)	47.0
Leakage current proportionality constant	1.60×10^{-3}
Leakage current T_0 (K)	64.0
Junction series resistance for 600 μm gain section (Ω)	8.0
Junction Fermi voltage (V)	0.8
Internal efficiency	0.85
Optical confinement (gamma)	0.02
a linear recombination term (s^{-1})	1.00×10^{8}
b bimolecular recombination term ($\text{cm}^3\,\text{s}^{-1}$)	1.00×10^{-10}
c Auger recombination term ($\text{cm}^6\,\text{s}^{-1}$)	1.10×10^{-28}
J_0 Transparency current density (A cm^{-2})	27.5
g_0 gain model parameter (μm^{-1})	0.28

By varying the currents applied to the separate tuning sections and repeating the procedure described above we can map out the lasing wavelength and threshold current over the full tuning range of the laser. In addition, models can be used to estimate the output power and static side-mode suppression ratio (SMSR). A method taking into account leakage current and thermal effects, such as due to Makino *et al.* [13], can give a good estimate of the output power even for currents well above the calculated threshold point. Note, however, that in our implementation we apply the Makino power estimation method to the lowest threshold longitudinal mode only and so we ignore the effect of mode jumps as the gain current is increased. Once the power in the cavity is known, the SMSR can be estimated from the difference in modal gain of the lasing mode and the mode with the next lowest threshold current by using the well known Fabry–Perot result [14]

$$\mathrm{SMSR} = \Delta(\Gamma g_{th})L \cdot \frac{P}{\gamma_m n_{sp} h\nu} \quad (3)$$

where P is the average power in the cavity, $\Delta(\Gamma g_{th})$ is the difference in threshold gain of the two competing modes, L is the cavity length, γ_m is the round trip loss seen by the main mode, n_{sp} is the inversion factor and $h\nu$ is the photon energy.

4 Experimental realisation and comparison

Fig. 7 shows a photograph of the top view of a DS-DBR chip. The cluster of eight contacts at the front of the device (right side of the Figure) are clearly visible as are the much larger contacts for the gain, phase and rear grating. Details of the device structure and fabrication are given at greater length elsewhere, albeit for a prototype device with a simpler front grating structure and hence a more limited tuning range [5]. The results presented here are for a device packaged in a standard 26-pin butterfly module.

In Fig. 8 we show the measured output spectrum of the device when one particular lasing mode has been selected. The device shows excellent single-mode behaviour with a SMSR in excess of 50 dB and a high output power of about 9 dBm in fibre. Fig. 9 shows the comparison between the measured tuning behaviour of the device and the tuning predicted by our transfer matrix model. The phase grating at the rear of the device was designed to consist of a comb of seven sharp reflection peaks, with a peak spacing of 6.8 nm. The wavelength centring of the comb was chosen such that the wavelength of each peak matched the Bragg wavelength of one of the gratings at the front. Each of the seven curves on the plot corresponds to the lasing wavelength being determined by one of the seven peaks in the rear reflector comb. Both total tuning range and the efficiency of tuning with injected current match well to the modelled result.

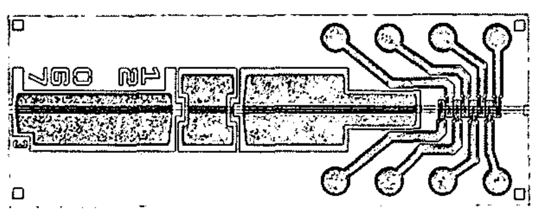

Fig. 7 *Top view of a DS-DBR chip*

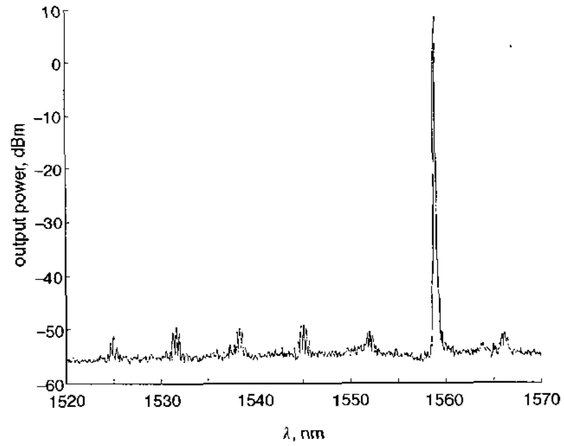

Fig. 8 *Measured output spectrum from a DS-DBR module*
Note the high side-mode suppression ratio

In Fig. 10 we show plots of the simulation results for the wavelength, output power, threshold current and SMSR for an ideal DS-DBR device as it is tuned. In each plot the horizontal axis labels the front contact into which current is injected while the vertical axis labels the current injected into the rear grating. The tuning separates into vertical bands or super-modes, each super-mode corresponding to the selection of one tuning sub-band by the front grating.

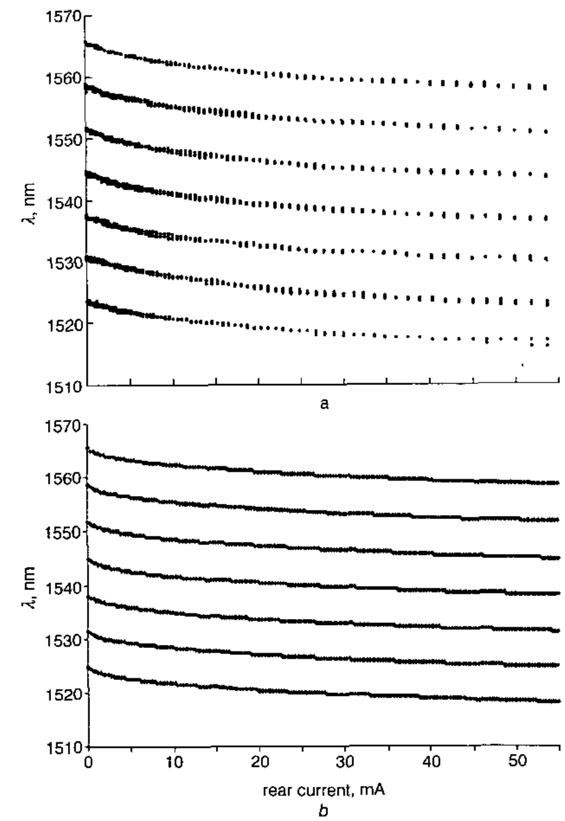

Fig. 9 *Comparison of measured and predicted tuning behaviour*
a Measured tuning behaviour
b Theoretical tuning prediction

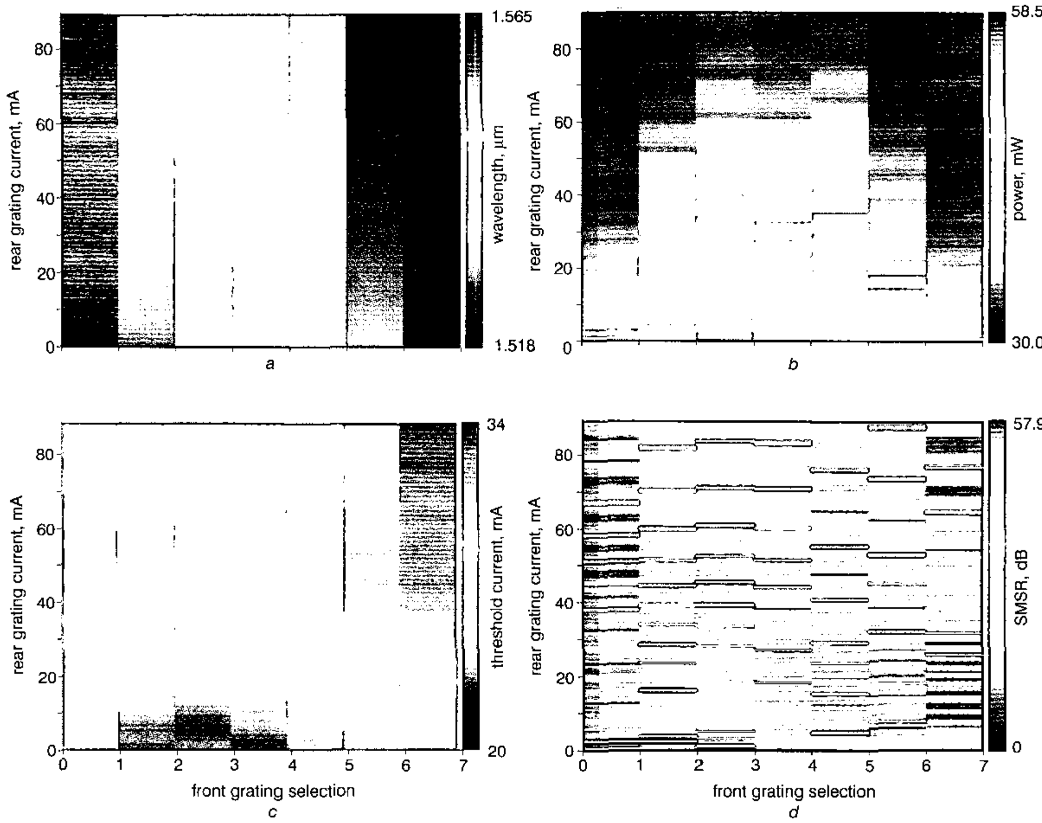

Fig. 10 *Contour plots of wavelength (a), output power (b), threshold current (c) and side-mode suppression ratio (d) obtained from the transfer matrix model of an ideal DS-DBR device*

The horizontal stripes within each super-mode correspond to the longitudinal modes of the laser cavity. The current range applied to the rear grating in the simulation was 0–90 mA, which was sufficient to give overlap between adjacent super-modes. For the choice of currents injected into the front gratings, it was observed that best results were achieved by driving the gratings in pairs and adjusting the current in order to track the front reflector together with the rear comb. This helped to improve the overlap between the front and rear reflection peaks as the rear was tuned. Using the rear current as a single control parameter in this way maintained a simple control algorithm. Although our model is somewhat idealised, the agreement with the experiment is good. The modelling shows quasi-continuous tuning over 50 nm (Fig. 10*a*) and the side-mode suppression ratios of 50 dB or more are realistic (Fig. 10*d*). The *L*(*I*) characteristics of the model are scaled by calibration, which in this case is a little optimistic, but nevertheless show the correct qualitative behaviour for output power (Fig. 10*b*) and threshold current (Fig. 10*c*) for a device of this style.

5 Conclusions

In this paper we have presented the modelling of a novel wideband tuneable laser design. We have employed an efficient, transfer matrix method to predict the behaviour of the device, including tuning behaviour and threshold current. In addition simple, phenomenological models can be used to extract the output power and static side-mode suppression ratio. This approach is fast enough to allow a wide exploration of the potential design space within a structured simulation environment and is an appropriate tool for design optimisation. The DS-DBR device has been fabricated and tested and demonstrated an impressive tuning range of 50 nm, as well as output powers of 8–9 dBm in fibre and good single-mode behaviour with a SMSR of better than 50 dB on 80 WDM channels with 50 GHz spacing.

6 References

1 COLDREN, L.A.: 'Monolithic tunable diode lasers', *IEEE J. Sel. Top. Quantum Electron.*, 2000, **6**, (6), pp. 988–998
2 ROBBINS, D.J, WHITBREAD, N.D., WILLIAMS, P.J., and RAWSTHORNE, J.R.: 'Design and optimisation of sampled grating DBR lasers for dense WDM networks'. Proceedings of ECOC 1998, Madrid, Spain, pp. 221–222
3 WOOD, S.A., PLUMB, R.G.S., ROBBINS, D.J., WHITBREAD, N.D., and WILLIAMS, P.J.: 'Time domain modelling of sampled grating tuneable lasers', *IEE Proc., Optoelectron.*, 2000, **147**, (1), pp. 43–48
4 SARLET, G., MORTHIER, G., BAETS, R., ROBBINS, D.J., and REID, D.C.J.: 'Optimisation of multiple exposure gratings for widely tunable lasers', *IEEE Photonics Technol. Lett.*, 1999, **11**, (1), pp. 21–23
5 REID, D.C.J., ROBBINS, D.J., WARD, A.J., WHITBREAD, N.D., WILLIAMS, P.J., BUSICO, G., CARTER, A.C., WOOD, A.K., CARR, N., ASPLIN, J.C., KEARLEY, M.Q., HUNT, W.J., BRAMBLEY, D.R., and RAWSTHORNE, J.R.: 'A novel broadband DBR laser for DWDM networks with simplified quasi-digital wavelength selection'. Presented at OFC 2002, Anaheim, USA, Paper ThV5
6 BJÖRK, G., and NILSSON, O.: 'A new exact and efficient numerical matrix theory of complicated laser structures: Properties of asymmetric phase-shifted DFB lasers', *J. Lightwave Technol.*, 1987, **5**, (1), pp. 140–146
7 PENDRY, J.B., and MACKINNON, A.: 'Calculation of photon dispersion relations', *Phys. Rev. Lett.*, 1992, **69**, (19), pp. 2772–2775
8 PENDRY, J.B.: 'Low energy electron diffraction' (Academic, London, 1974)
9 KOGELNIK, H., and SHANK, C.V.: 'Coupled-wave theory of distributed feedback lasers', *J. Appl. Phys.*, 1972, **43**, pp. 2327–2335

10 CARROLL, J., WHITEAWAY, J., and PLUMB, D.: 'Distributed feedback semiconductor lasers' (IEE, London, 1998)
11 HAKKI, B.W., and PAOLI, T.L.: 'Gain spectra in GaAs double-hetrostructure injection lasers', *J. Appl. Phys.*, 1975, **46**, (3), pp. 1299–1306
12 SHIMIZU, H., KUMADA, K., YAMANAKA, N., IWAI, N., MUKAIHARA, T., and KASUKAWA, A.: '1.3 μm InAsP *n*-type modulation-doped MQW lasers grown by gas-source molecular beam epitaxy', *IEEE J. Sel. Top. Quantum Electron.*, 1999, **5**, (3), pp. 449–456
13 MAKINO, T., EVANS, J.D., and MAK, G.: 'Maximum output power and maximum operating temperature of quantum well lasers', *Appl. Phys. Lett.*, 1997, **71**, (20), pp. 2871–2873
14 MORTHIER, G., and VANKWIKELBERGE, P.: 'Handbook of distributed feedback laser diodes' (Artech House, Boston, 1997)